Experimental study of a mechanically ventilated double-skin façade with venetian sun-shading device: A full-scale investigation in controlled environment

V. Gavan, M. Woloszyn, F. Kuznik, J.-J. Roux

Experimental study of a mechanically ventilated double-skin façade with venetian blinds: A full-scale investigation in controlled environment

Valentin Gavan*

CETHIL, UMR5008, CNRS, Université de Lyon, Lyon, F-69003, INSA-Lyon, Villeurbanne, F-69621, Université Lyon1, Lyon, F-69622, France

Centre Scientifique et Technique du Bâtiment, CSTB, Champs sur Marne, F-77447 Marne-la-Vallée, France

Monika Woloszyn

CETHIL, UMR5008, CNRS, Université de Lyon, Lyon, F-69003, INSA-Lyon, Villeurbanne, F-69621, Université Lyon1, F-69622, France

Frédéric Kuznik

CETHIL, UMR5008, CNRS, Université de Lyon, Lyon, F-69003, INSA-Lyon, Villeurbanne, F-69621, Université Lyon1, F-69622, France

Jean-Jacques Roux

CETHIL, UMR5008, CNRS, Université de Lyon, Lyon, F-69003, INSA-Lyon, Villeurbanne, F-69621, Université Lyon1, F-69622, France

* Corresponding author. Tel.: +33-472-438-468; Fax: +33-472-438-811
Email address: valentin.gavan@insa-lyon.fr (Valentin Gavan).

Experimental study of a mechanically ventilated double-skin façade with venetian blinds: A full-scale investigation in controlled environment

Valentin Gavan[a,b,*] Monika Woloszyn[a] Frédéric Kuznik[a] Jean-Jacques Roux[a]

[a] CETHIL, UMR5008, CNRS, Université de Lyon, Lyon, F-69003, INSA-Lyon, Villeurbanne, F-69621, Université Lyon1, Lyon, F-69622, France

[b] Centre Scientifique et Technique du Bâtiment, CSTB, Champs sur Marne, F-77447 Marne-la-Vallée, France

Abstract

The aim of this article is to present results of an experimental campaign performed on a full scale facility provided with a double-skin façade. The behaviour of this architectural concept is tested under controlled climatic conditions. A summer case is scrutinised under different configurations: variation of the airflow through the double-skin façade and different angle of the solar shading device. This paper describes the experimental conditions, as well the test facility and the tested façade element. The results show the temperatures of the test cell and the façade and how they depend on the climatic conditions and the blind blade angles. One objective of this research was to measure and provide extensive data set detailing air and surface temperatures on the double-skin façade, together with airflow rates and air velocities. The experiments are fully described so that the results can be used for the validation of numerical models dealing with ventilated double-skin façades with venetian blinds.

Keywords: double-skin façade, full-scale experiment, mechanical ventilation, venetian blinds.

[*] Corresponding author. Tel.: +33-472-438-468; Fax: +33-472-438-811
Email address: valentin.gavan@insa-lyon.fr (Valentin Gavan).

1 Introduction

Double-skin façades are highly technological building components which are deployed especially for office buildings in order to satisfy special requirements. Although the double-skin façade (DSF) concept is not new, there is a growing tendency from the architects to use it. In new architectural projects, the DSF are designed to fulfil several envelope functions, such as thermal and acoustic insulation, optimization of natural lighting and improvement of ventilation system. Given that the study of DSF constructions has appeared during recent years, a satisfying level has not been yet achieved and the lack of knowledge is still present.

The DSFs were studied in the past years to improve their capacities headed for the energy performance simultaneously with preservation of the thermal and visual comfort. In addition to the envelope itself (façade), DSF have a second glazed layer (generally without a structural function) placed at a certain distance from the inner layer (Streicher, 2005). These two panes of glass act as an insulation between outside and inside enabling the air to circulate the cavities of the façade. The zone positioned between these two layers is named buffer zone, channel or air gap and is generally ventilated. Since the distance between the glass layers goes from a few centimetres to over one meter, this significant air volume can be used various ways according to climatic conditions, hours of occupation, orientation, type of construction and HVAC system. Its temperature is influenced by solar radiation, outside temperature, presence of shading systems.

Although numerous papers describe different configurations of DSF, experimental results under controlled climatic environment are rarely given. Measurements are very often carried out under real weather conditions where there is a little or no control of the key environmental factors (Pasquay, 2004), (Park et al., 2004), (Stec and Van Paassen, 2005), (Corgnati et al., 2007). All these experiments treat different façade configurations. Results of measurements are used for validation and enhancement of developed models. Generally, these results are employed to improve DSF performance at the design stage.

In (Pasquay, 2004) several high-rise naturally-ventilated DSF on real buildings are monitored. In (Stec and Van Paassen, 2005) three main experiments are evaluated, one in a small-scale laboratory facility and two under real weather conditions. The small-scale test cell measurements are performed to validate a simplified DSF model without an influence of wind and solar radiation. Measurements under real weather conditions were used to validate the building model coupled with the DSF. In (Corgnati et al., 2007) the authors evaluate extensively the operation of a DSF integrated with HVAC strategies. The air is drawn from the room and flows through the façade to an air treatment unit. The main inconvenient of this strategy is that during the winter, due to the occupants, condensation may appear on the outer glazing of the façade.

The major inconvenient of this large variety of experimental situations reside generally in the different climatic conditions, as well as building or DSF characteristics. In this case, aiming inter-building and/or inter-façade comparisons became very complicated.

2 Experimental set-up

The first part of this paper is dedicated to an extensive description of the experimental set-up. The second chapter deals with the results obtained during the experimental campaign. Finally, conclusions are given in the last part of the paper.

2.1 Minibat test cell

The study of thermal characteristics or influence of a system connected to a building structure, requires reliable and detailed experimental data. However, the consistency of such measurements can only be acquired through controllable experimental environment, situation constituting the essence of the climatic test cell called Minibat. Used intensively for the last years to validate zone and CFD models or to measure pollutant, Minibat cell was upgraded recently to a new potential, the assessment of a double-skin façade system.

The Minibat experimental facility is composed by two identical test cells (rooms), each one with the dimensions L × W × H = 3.1 m x 3.1 m x 2.5 m (Figure 1). Throughout measurements, the door between the tests cells was sealed and only the data from test cell 1 were considered, henceforth called test cell. Five walls of the test cell are in contact with a thermal buffer zone with controlled temperature. The composition of the walls is given in Table 1. The thermophysical properties of the materials are summarized in Table 2. To create a homogeneous and regular volume of air inside the thermal buffer zone, a distribution air network is installed. The air diffusers are installed in the upper part of the thermal buffer zone and air outlets in the lower part. The air temperature inside the thermal buffer zone is entirely controlled with an accuracy of ±0.5°C. The sixth face of the test cell, where the DSF is installed, is in contact with a weather generator capable of simulating the outdoor conditions (temperature and solar radiation). An air treatment unit controls the air temperature in the weather generator. The average air temperature can vary between 0°C and 40°C with an accuracy of ±1.5°C.

2.2 Large scale solar simulator

The large scale solar simulator installed in the Minibat test cell provides a source of artificial solar radiation for irradiating the test façade surface (see Figure 1). The solar simulator is designed to test elements W × H = 3.1 m x 3.1 m. The lamps are physically separated from weather generator by a glass pane. Thus, the separation between solar and weather generator allows measurements with different scenarios (summer, winter, middle season configuration), without deterioration of the lamps characteristics. This environment that adjoins the front irradiated surface of the façade and the solar simulator corresponds to outdoor environment.

The solar radiation is simulated using twelve 1000W CSI lamp (a gaseous discharge lamp of metal halide type, CSI meaning compact source iodide). Figure 2 shows the comparison between the CSI spectrum and the solar spectrum (Allard et al., 1987). Then, the lamps are capable of producing a radiative spectrum close to the solar spectrum. The lamps are installed in three rows of four lamps in front of the weather

generator (Figure 3). Every lamp is electrically controlled by a supervising unit which allows the functioning of different combination of lamps. During our tests all the lamps were switched on.

2.3 Double-skin façade

As a result of a literature review, the more conventional façade element comprising a single storey "box-window" type is selected in our investigation (Loncour X. et al., 2004). In this respect, a full sized double-skin façade incorporating a sun-shading blind was constructed and installed in the Minibat test cell.

The double-skin façade, presented in Figure 4, is made of two aluminium frames: external and internal. The internal is composed of one fixed part (W × H = 2.8 m x 2.3 m) while the external one is divided into two parts that can be separately opened. The aluminium frame (6 cm thick by 10 cm of width) is a specially designed 3 cell formation limiting thermal bridges. The glass panels, separated by a gap of 20 cm, are two simple clear glazing without a surface treatment. The glass area is W × H = 1.3 m × 1.93 m (2 panes) for the external pane and W × H = 2.8 m × 1.93 m (one pane) for the internal pane. The outer skin was designed to be opened and closed for easy installing the measurement devices and directing the solar blinds.

The DSF includes four openings for ventilation (W × H = 2.6 m x 0.04 m). They cover the whole width of the façade, at top and bottom of each of the two glass panels. Thus, various ventilation configurations of double-skin can be tested by simple obstruction of these openings.

The sun-shading devices, commonly used in practice and installed for these experiments, are venetian blinds placed in the middle of the channel. Since the sun-shading device is motor driven, the blinds can be oriented automatically during the tests, from the exterior of the façade. The orientation is representing an imposed angle (β) between 0° and 90°. The 0° angle corresponds to horizontal completely open blinds. The 90° angle corresponds to completely closed blinds facing the solar simulator. Made of aluminium, tested sun-shading blades are 2.5 cm of width (total sun-shading system dimension is W × H = 2.8 m ×

2.3 m), 0.21 mm thick and with a weight of 699 g/m² of weight. The chosen colour of the blinds is yellow gloss. Table 3 summarizes the DSF properties.

The DSF is exposed to the controlled climatic conditions (temperature and solar radiation), provided by the weather generator and the solar simulator. In order to represent precisely a mechanically ventilated façade and ensure accurate airflow control a special air supply system was designed (Figure 5). This system is connected to the lower ventilation opening of the DSF. It is composed of a ventilator which blows the air into a convergent diffuser by the intermediate of a duct (Figure 5a). A differential pressure flowmeter is installed inside this duct to measure accurately the airflow blown by the ventilator into the air channel of the façade (Figure 5c). Preliminary tests show that the velocity at the diffuser outlet is nearly uniform.

2.4 Metrology

The metrology installed on the experimental facility is composed in two systems, one for the test cell and the other for the DSF. Both measurement units are composed of 70 thermocouples and 7 RTD sensors, one inline flowmeter and one pyranometer. Table 4 summarises the sensors properties. The entire test cell is equipped with type-K thermocouples on its interior and external surfaces (facing inside and facing thermal buffer zone). 9 thermocouples are located on each face of five walls in order to obtain the mean surfaces temperatures.

The DSF airflow measurement system is composed of two differential pressure devices (two blades, thus limiting the differential heads and turbulences) and a sensor box with the differential pressure elements (Figure 5c). These two pressure elements have a distribution of apertures on the airfoil permitting the control of the average airflow (by averaging the differential pressures). The pressure transmitters working with a differential probe are configured with a square root function. Via this function, and from the differential pressure, the transmitter calculates air velocity and/or airflow in the duct, and thus in the DSF.

The DSF itself is instrumented using thermocouples, distributed on all the elements of the façade (Figure 6). Type-T thermocouples with flattened joint are used here for a better contact with the glass surface. Among these sensors (Table 4), 15 thermocouples are affected for the glass surface temperatures and 10 for air temperatures (Figure 6). All the thermocouples installed in the DSF are shielded to the solar simulator radiation using a special paint. This paint is Labsphere's Spectraflect.

Air velocity transducers are also installed. The sensors are TSI 8475 Air velocity Transducer. They sensors are selected to measure air velocities within the mechanically ventilated cavity. Thus, four air velocity transducers were used for the measurements. The transducers were located at the middle height (+1.15m) and in the upper part (+2.1m) of the façade cavities (external and internal air channels). Each air velocity transducer is suspended vertically in the cavity with the sensors facing the upward airflow. The uncertainties concerning velocity measurements are given in Table 4.

The test cell sensors are connected to a multiplexing station composed of 10 acquisition cards, each one having 39 inputs. Measurements are then carried out using a multimeter Keithley 2700. DSF sensors are connected to a dedicated Multimeter/Data Acquisition System. Acquisition and recording of the data are done by a computer station using Labview software.

2.5 Experimental procedure and preliminary results

2.5.1 Experimental procedure

Every test consists in setting up parameters of the test cell facility (boundary conditions) and DSF. Simultaneously, the solar simulator is switched on and synchronized with the acquisition system. The time delay between two measurements is 300 s (i.e. a measurement frequency of 0.003 Hz). The test cell reaches the steady state condition after 48 hours when the DSF is ventilated, respectively 72 hours with no airflow in the DSF. All the values presented in this paper were obtained averaging 100 values recorded at steady state. Comprehensive and more detailed information about the configurations are given in Figure 7.

2.5.2 Thermal buffer zone

Given that the thermal buffer zone temperature around all the five boundaries of the test cell is accurately controlled, it is possible to test several cases. Among these, a main scenario was selected for the tests. This scenario is represented by a summer situation which is representative of the hot period. This configuration of the thermal buffer zone simulates the cell test in contact with adjacent rooms at constant temperature. Therefore, the temperature of the thermal buffer zone is fixed according to the studied case. Thus, the air temperature of the thermal buffer zone was fixed at 26°C (Figure 7).

2.5.3 Weather generator

During tested scenario, the air temperature inside the weather generator is fixed at 32°C (Figure 7). The weather generator oscillation around the temperature setpoint is reduced to approximately ±0.2-0.3°C for all configurations, which confirms the stability of the weather generator regulation system.

2.5.4 Solar simulator radiation results

During all the tests, the solar simulator is unchanged constant. The orientation angle of these lamps is chosen following preliminary tests, to uniformly irradiate the DSF structure.

To obtain uniform radiation repartition, the lamps are redirected until reaching a homogenous radiative solar flux on the external DSF glass pane. The measurements are realised simultaneously on a virtual grid (Figure 8) on the external and the internal glass pane. With these measurements, is possible to evaluate the values of solar radiation in different location of the DSF. Figure 9 presents the solar irradiation isovalues on the external glazing after the reorientation of the lamps. External glass sheet receives the most significant part of the radiation of solar simulator spots. The reorientation of lamps allows to improve and to normalize the initial regions with a high irradiation (in real case, the sun is sufficiently far to act as punctual source and to radiate uniformly). Figure 10 presents the same direction as Figure 9, but

the measures were taken on the internal DSF glass pane. Figure 10 shows as well, that a significant part of the solar radiation is absorbed or reflected by the glass panes or by the venetian blinds of the DSF. Figure 11 summarises all the internal solar radiation measurements for blinds angles (β) varying from 0 to 90 degrees. For convenience, the measured values on different location of the façade glass (exterior and interior, Figure 9 and Figure 10) are averaged. Thus, Equation (1) defines the shading coefficient ζ, function of the radiative flux on the DSF external and the internal glass sheet. This shading coefficient describes the amount of solar radiation which is stopped by closing progressively the blinds.

$$\zeta = \frac{E_{S-ext}}{E_{S-\mathrm{int}}} \qquad (1)$$

For each change of the blinds angle the average irradiation is decreasing by approximately 50% comparing to previous angle (for example, between horizontal blinds and 30° blinds). Moreover, for completely closed blinds (90°), since the theoretical transmittance is equal to 0, the first consequence can be that no radiation will enter inside test cell. But with multiple reflections and solar radiation leakage regions of the façade, the test cell receives solar radiation.

2.5.5 DSF airflow and air velocities results

In this part the airflow and the air velocities inside the DSF are analysed. The air velocities are analysed by the intermediate of a coefficient. This coefficient (see equation 2) is a function of measured air velocities inside the DSF gaps, at middle height. As well, this coefficient depends of the ventilation opening surface and of the imposed airflow at the entering of the DSF.

$$\Psi = \frac{v_{H=1.15} \cdot S_{vent}}{Q_v} \qquad (2)$$

Figure 12

3 Results

In this part, results obtained from the measurements are detailed. Various scenarios are considered.

3.1 Temperature results

The scenario is characterized mainly by the weather generator air temperature fixed at 32°C (a hot summer day) and the buffer zone temperature fixed at 26°C (the test cell is supposed to be in contact with a air-conditioned zone). Under these aspects, several configurations are scrutinised: different airflows combined with different orientation of the shading device. In our case, the presence of venetian blinds allows to vary the angle between 0° (completely opened blinds) and 90° (completely closed blinds). The airflow range varies between 0 and 600 m^3/h corresponding to 0-193 m^3/h for one meter of façade. All the tested configurations are presented in Figure 7.

Table 5 presents the totality of the boundary conditions of the test cell facility; the temperatures of the thermal buffer zone air volumes (North and South face, Ceiling and Floor). The fluctuations between the setpoint and the temperature in the thermal buffer zone, on the North, South and top air volumes are around 1.3°C. For the bottom face of the thermal buffer zone, in contact with the floor, the temperature recorded during the measurements is in the region of 22°C. Table 6 presents the temperatures recorded on interior surface of the walls of the test cell. For convenience, the 9 thermocouples recordings are time averaged and only one value is presented for every wall. Similarly to thermal buffer zone, the walls temperatures are averaged from 100 values recorded at steady state. For example, during the measurements with the completely opened blinds, increasing the airflow in the façade is decreasing the walls surface temperatures (North, South, Ceiling and Floor). For the East wall (the back wall of the test cell) the temperature is relatively constant for all airflows. This fact is due to the solar radiation passing through the façade, irradiating the wall surface. Modifying the blades angles, the solar direct flux through

the DSF is reduced and the consequence is observed on the back wall surface temperature. This wall surface temperature decreases simultaneously with the increasing of the blinds angle.

Installing thermocouples in different points of the DSF (Figure 6) and inside test cell (6 Pt100 sensors are installed to measure the vertical temperature profile), a temperature evaluation is realised for different location. Consequently, every sensor will record the temperature of the near environment (surface or air). Thus, for measured configurations (airflow and blades angle) top and bottom recordings of test cell and DSF layers were averaged at steady state. Table 7 shows these temperatures for all the summer configurations. In the light of this situation is possible to calculate a temperature difference top-bottom for each element. This vertical temperature difference of the DSF elements, particularly for air temperatures, is important to be evaluated. This evaluation shows if the DSF can increase sufficiently the air temperature, air that can be provided for ventilation. This situation is supposed advantageous during middle or moderate cold season.

Figure 13 shows that blinds angle are highly influencing the temperature regimes DSF and test cell. The test cell air temperature is more influenced by the blinds angles than by the airflow. Thus, closing progressively the blades, a more consequent decrease of temperature is produced inside the test cell than by doubling the airflow.

For both mechanical ventilation and zero ventilation through the DSF, blinds temperature is superior to all other temperatures (air and surfaces of the DSF). This temperature difference vary proportionally with the blinds angles, from approximately 1.5°C for blinds at 0°, respectively to 3°C for blinds at 90°(closed sun-shading system). The blinds increased temperature is due to the progressive interception of the solar radiation. Thus, more the blinds are closed more their temperature is increasing.

Figure 14 shows an outlook of the entire set of temperature measurements for the test cell. Measured temperature inside test cell varies few for angles superior to 60. Subsequently to our measurements and strictly thermo-energetic, hot season strategies with angles superior to 60° (even with important airflow in the DSF) cannot be considerate giving a thermally sufficient impact. Thus, since a 60° angle gives a

similar decrease of temperature as a 90° angle (closed blinds), a lower angle is more suitable due to his higher daylighting potential.

3.2 DSF energy efficiency results

This consequence presented in Figure 14 is reinforced calculating the energy efficiency of the DSF (see equation 3). This coefficient is a measure of the energy "removed" from the test cell by the airflow imposed in the DSF. This coefficient depends of the measured air temperatures at the lower and upper ventilation openings of the DSF. Moreover, this coefficient is correlated with the solar simulator radiative flux and the glass surface of the DSF.

$$E = \frac{Q_m \cdot c_p \cdot (T_{out} - T_{in})}{E_{S-ext} \cdot S_g} \qquad (3)$$

Therefore, Figure 15 presents the energy efficiency function of different airflow. Increasing more the blinds angle is not traduced by removing more heat from the façade. For a small airflow (200 m^3/h) the energy efficiency is nearly constant for all angles excepting complete opened blinds. The maximum of energy efficiency is for blinds angle of 45°. After this value, the trend is directed downward which makes that a 60° angle to be equivalent thermo-energetically with a 30° angle. From a natural lighting perspective, small angles can lead to better use of daylight inside allowing more solar radiation to pass towards the room. This limited blinds inclination due to thermal aspects can simplify further the DSF control (high glazed surface with bad consequences on thermal comfort, but with good effects for visual comfort) and thus giving more access to natural light.

4 Conclusions

In order to investigate glazed building envelope, an experimental research has been carried out with double-skin façades. This study allows measurements of double-skin façades, under controlled thermal

and radiative environment. The tests concern the behaviour of the test cell provided with a double-skin façade during the hot season characterised by different set-ups (blinds angle and ventilation).

These experimental campaigns enable us to evaluate precisely the thermal behaviour of a room provided with a double-skin façade, comparing to real building monitoring. However, this entire set of experimental results enables to carry out validation of DSF models. Thus, this extensive data set (boundary conditions, walls surface temperature, DSF temperatures, etc.) can provide a practical resource for further research and for use by building designers and modellers.

In order to validate the use of double-skin façades, further investigations are needed. Various external conditions must be tested to evaluate the gain during spring, autumn. As well, numerical simulations must be carried out, in order to investigate the behaviour for real buildings. The thermal and visual aspects are to take into account simultaneously.

References

Allard F., Brau J., Inard C., Pallier J.M., 1987. Thermal Experiments of Full-Scale Dwelling Cells in Artificial Climatic Conditions. Energy and Buildings 10 (1987) 49-58.

Corgnati S.P., Perino M., Serra V., 2007. Experimental assessment of the performance of an active façade during actual operating conditions. Solar Energy 81 (2007) 993-1013.

Loncour X., Deneyer A., Blacso M., Flamant G., Wouters P., 2004. Les double façades ventilées. Classification & Illustration des concepts de façades. Centre Scientifique & Technique de la Construction, Département Physique du Bâtiment, Climat intérieur & Equipements, Belgique.

Park C., Augenbroe G., Sadegh N., Thitisawat M., Messadi T, 2004. Real-time optimization of a double-skin façade based on lumped modelling and occupant preference. Building and Environment 39 (2004) 939 – 948.

Pasquay T., 2004. Natural ventilation in high-rise buildings with double façades, saving or waste of energy. Energy and Buildings 36 (2004) 381–389.

Poirazis H., 2006. Double skin façade literature review. IEA Task34.

Stec W.J., Van Paassen A.H.C., 2005. Symbiosis of the double skin façade with the HVAC system. Energy and Buildings 37 (2005) 461–469

Streicher W., 2005. Bestfaçade - Best Practice for Double Skin Façades EIE/04/135/S07.38652. WP 1 Report State of the Art.

Nomenclature

β	Blinds angles [°]
ζ	Shading coefficient [-]
E_{S-ext}	Solar simulator flux measured on the external DSF glass [W/m²]
$E_{S-\mathrm{int}}$	Solar simulator flux measured on the internal DSF glass [W/m²]
E	Energy efficiency [-]
Q_m	Mass flow [kg/s]
c_p	Specific heat capacity [J/kg K]
T_{out}	Air temperature in the upper part of the DSF [°C]
T_{in}	Air temperature in the lower part of the DSF [°C]
S_g	Glass surface of the DSF [m²]

Table 1. Wall composition (from the interior of the test cell to the thermal buffer zone)

Wall	**Material**	**Thickness [mm]**
Floor	Cellular concrete	200
Vertical wall	Plasterboard	10
	Polystyrene	50
	Plasterboard	10
	Agglomerated wood	50
Ceiling	Plasterboard	10
	Plywood	8
	Mineral wool	55
	Wood	25

Table 2. Thermophysical properties of the envelope

Material	**Conductivity**	**Capacity**	**Density**
	[W/m^2°C]	**[J/kg°C]**	**[kg/m^3]**
Plasterboard	0.35	1620	817
Agglomerated wood	0.136	1640	544
Plywood	0.11	1600	417
Polystyrene	0.04	1380	25
Mineral wool	0.06	1000	72
Siporex concrete	0.16	1000	368

Table 3. Double-skin façade properties

Layer	Dimensions		Transmittance	Absorptivity	Reflectivity
	Width	Height			
	[m]	[m]	[%]	[%]	[%]
External DSF glass pane	2.6	2.3	0.82	0.11	0.07
Venetian blade	2.6	-	0	0.1	0.9
Internal DSF glass pane	2.6	2.3	0.82	0.11	0.07

Table 4. Sensor characteristics

Sensor	**Type**	**Precision**
Thermocouple	K	±0.3°C
Thermocouple	T	±0.6 °C
Thermocouple	T	±0.6 °C
Platinum RTD	Pt100	±0.2 °C
Platinum RTD	Pt100	±0.2 °C
Flow rate	-	±0.5 %
Air velocity transducer	TSI Omni directional	±3 % if T $\in$ [20°C; 26°C] ±3 % + 0.5% per °C of reading if T $\notin$ [20°C; 26°C]

Table 5. Boundary conditions

β	Q_v	Weather generator	Thermal buffer zone			
			North	Top	South	Bottom
	[m^3/h]	[°C]	[°C]	[°C]	[°C]	[°C]
0	0	32.3	24.9	25.9	25.4	21.5
0	200	32.2	24.7	25.7	25.2	22.0
0	400	32.2	25.5	26.3	25.8	21.8
0	600	31.9	25.5	26.3	25.7	22.2
30	0	32.3	25.1	26.0	25.4	21.7
30	200	32.2	24.9	25.8	25.2	22.2
30	400	32.1	25.6	26.2	25.7	21.6
30	600	31.8	25.2	26.0	25.5	22.2
45	0	32.3	24.9	25.8	25.2	21.9
45	200	32.2	25.0	25.8	25.2	22.2
45	400	32.2	24.7	25.6	25.1	21.8
45	600	31.8	25.2	25.8	25.4	22.3
60	0	32.3	24.8	25.6	25.1	22.1
60	200	32.2	24.8	25.5	25.1	22.2
60	400	32.1	24.9	25.6	25.1	22.2
60	600	31.9	24.8	25.4	25.0	22.3
closed	0	32.3	25.0	25.8	25.3	22.0
closed	200	32.2	25.4	25.9	25.5	22.1
closed	400	32.2	25.9	26.6	26.1	23.0
closed	600	31.9	24.9	25.5	25.0	22.3

Table 6. Inside surface wall temperatures

β	Q_v	Walls indoor surface temperature				
		North	Ceiling	South	Floor	East
	[m^3/h]	[°C]	[°C]	[°C]	[°C]	[°C]
0	0	37.3	38.7	37.4	37.8	41.2
0	200	36.7	38.0	36.8	37.2	41.0
0	400	36.2	37.4	36.4	36.7	40.2
0	600	36.2	37.6	36.3	36.5	40.3
30	0	35.5	37.4	35.5	35.6	37.6
30	200	34.2	35.8	34.2	34.4	36.2
30	400	33.4	34.8	33.4	33.4	35.0
30	600	33.7	35.2	33.7	33.9	35.6
45	0	34.1	36.0	34.1	34.1	35.2
45	200	33.0	34.5	33.0	33.1	34.3
45	400	33.0	34.4	33.0	33.1	34.6
45	600	32.0	33.2	31.9	32.0	32.7
60	0	33.2	35.1	33.1	33.1	33.8
60	200	32.0	33.5	32.0	32.0	32.8
60	400	31.9	33.1	31.8	31.9	32.7
60	600	30.8	31.9	30.7	30.7	31.0
closed	0	32.7	34.5	32.5	32.5	32.9
closed	200	31.1	32.5	31.1	31.0	31.3
closed	400	31.7	32.8	31.6	31.5	32.0
closed	600	30.4	31.5	30.3	30.3	30.5

Table 7. DSF and test cell vertical temperature difference.
Bottom = +0.2m; Top = +2.1m

β	Q_v	External glass		External air channel		Blinds		Internal air channel		Internal glass		Test cell	
		Bottom	Top	Bottom	Top	Bottom	Top	Bottom	Top	Bottom	Top	Bottom	Top
	[m^3/h]	[°C]		[°C]		[°C]		[°C]		[°C]		[°C]	
0	0	35.4	39.3	34.5	41.9	35.5	42.7	33.4	42.4	37.8	42.1	37.4	39.5
0	200	35.3	38.3	34.6	38.1	35.5	38.8	34.1	38.5	36.9	40.2	36.5	38.9
0	400	35.0	37.5	34.4	36.2	35.2	37.9	34.0	36.8	36.5	39.3	36.2	38.3
0	600	35.3	37.5	34.4	36.0	35.8	37.5	34.3	36.6	36.6	39.1	36.1	38.4
30	0	35.2	40.1	34.2	43.7	35.0	45.4	33.0	43.6	36.2	41.6	35.4	38.0
30	200	35.6	39.0	34.6	39.3	35.8	40.5	34.0	39.5	35.4	39.2	34.0	36.0
30	400	35.5	38.2	34.5	37.2	36.3	40.5	34.1	36.6	35.0	37.8	32.9	35.1
30	600	35.7	38.0	34.6	36.6	36.6	38.4	34.3	36.8	35.5	37.9	33.6	35.3
45	0	35.1	40.6	34.2	44.7	34.7	46.4	33.0	44.1	35.3	41.0	33.6	36.6
45	200	35.5	39.1	34.4	39.4	35.6	40.8	33.8	39.5	34.7	38.4	32.4	34.6
45	400	35.7	38.4	34.6	37.3	36.4	40.7	34.1	36.6	34.9	37.6	32.5	34.4
45	600	35.9	38.4	34.8	36.9	36.8	39.2	34.4	36.4	34.7	36.8	31.1	33.2
60	0	35.0	40.9	34.0	44.9	34.8	46.6	32.9	44.1	34.7	40.5	32.5	35.7
60	200	35.5	39.5	34.3	39.5	35.6	41.4	33.7	39.5	34.1	37.8	31.1	33.5
60	400	35.8	38.8	34.5	37.4	36.4	41.3	34.1	36.1	34.3	36.8	31.0	33.2
60	600	36.1	38.9	35.0	36.8	36.8	39.5	34.5	36.0	34.1	35.9	29.6	32.0
closed	0	35.0	40.9	34.1	44.8	34.8	46.3	33.2	43.6	34.3	39.8	31.8	34.9
closed	200	35.4	39.5	34.1	39.3	35.4	41.8	33.6	39.2	33.5	37.0	29.9	32.5
closed	400	35.9	39.1	34.5	37.4	36.4	41.2	34.2	36.1	34.1	36.4	30.5	32.7
closed	600	36.3	38.9	34.9	36.7	36.7	39.5	34.5	35.8	33.9	35.5	29.1	31.5

Figure 1. Test cell facility scheme: 1, cooling unit; 2, weather generator; 3, double-skin façade; 4, protection glass of the solar simulator; 5, test cell; 6, concrete; 7, air blowing plenum; 8, solar simulator's heat removal ventilators; 9, air extraction plenum; 10, HVAC unit of the buffer zone; 11, solar simulator; 12, controlled buffer zone. (Metric units)

Figure 2. Comparison of a CSI simulator spectrum with solar spectrum

Figure 3. Large scale solar simulator. (Metric units)

Figure 4. DSF section view: 1, 6 mm glass layer; 2, motorized solar protection; 3, metallic support; 4, solar protection action box; 5, concrete beam; 6, aluminium frame; 7, pane opening articulation; 8, ventilation openings. (Metric units)

Figure 5. Double-skin façade air supply system. (Metric units)
a) Section view. b) Plan view. c) Flowmeter

Figure 6. Thermocouples position on double-skin façade elements. (Metric units)

Figure 7. Measurements configurations

Figure 8. Solar insulation measure grid (external and internal glass). (Metric units)

Figure 9. Solar simulator insolation distribution on the external glass pane

Figure 10. Solar simulator insolation distribution on the internal glass pane ($\beta=0°$)

Figure 11. Shading coefficient of the DSF function of different blinds angle

Figure 12. Middle height air velocities inside the façade cavities
a) External cavity; b) Internal cavity;

Figure 13. Double-skin façade temperature profile.
a) Blinds at 0° angle (completely opened); b) Blinds at 30° angle; c) Blinds at 45° angle;
d) Blinds at 60° angle; e) Blinds at 90° angle (completely closed);

Figure 14. Test cell air temperature

Figure 15. Energy removed from the test cell

Figure 1. Test cell facility scheme: 1, cooling unit; 2, weather generator; 3, double-skin façade; 4, protection glass of the solar simulator; 5, test cell; 6, concrete; 7, air blowing plenum; 8, solar simulator's heat removal ventilators; 9, air extraction plenum; 10, HVAC unit of the buffer zone; 11, solar simulator; 12, controlled buffer zone. (Metric units)

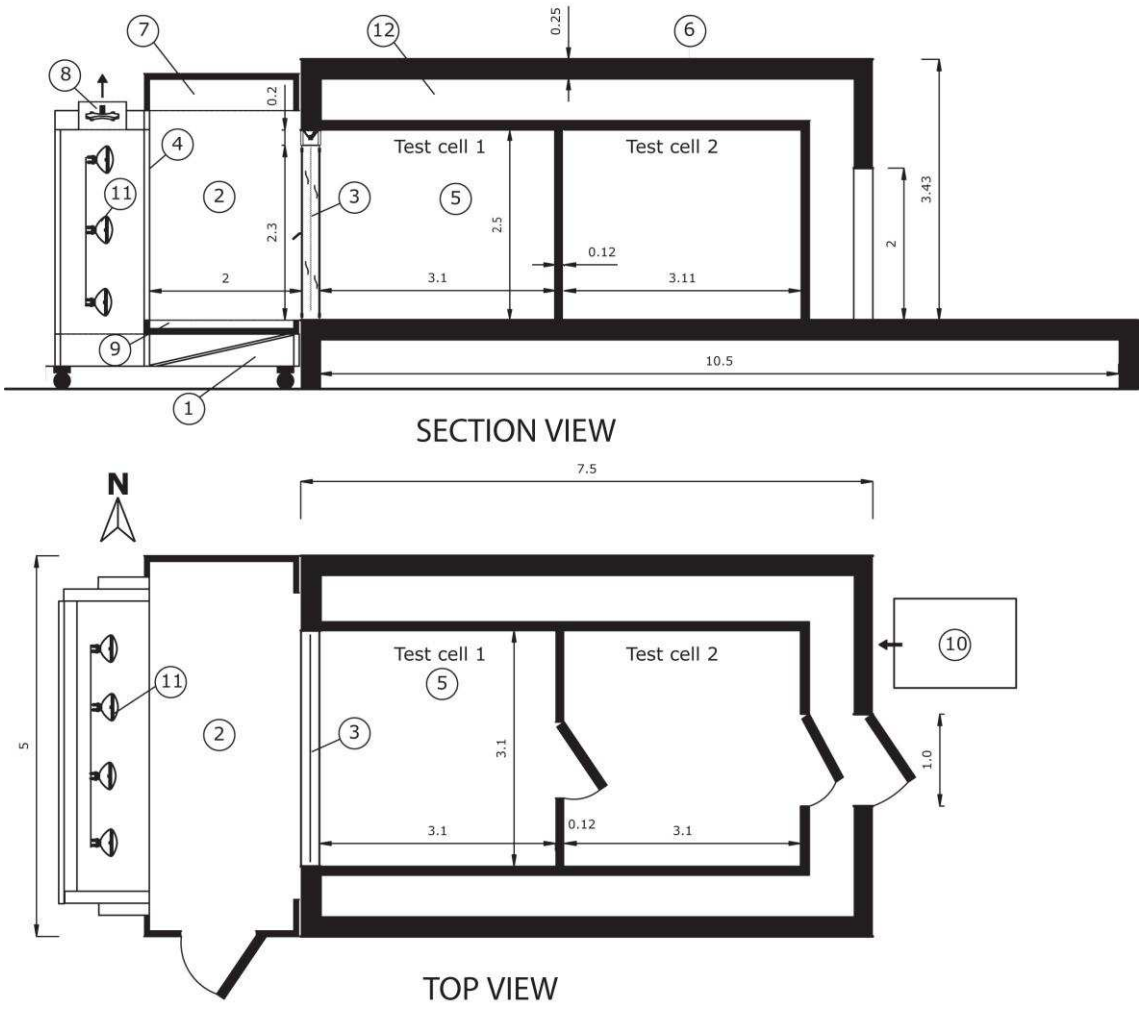

Figure 2. Comparison of a CSI simulator spectrum with solar spectrum

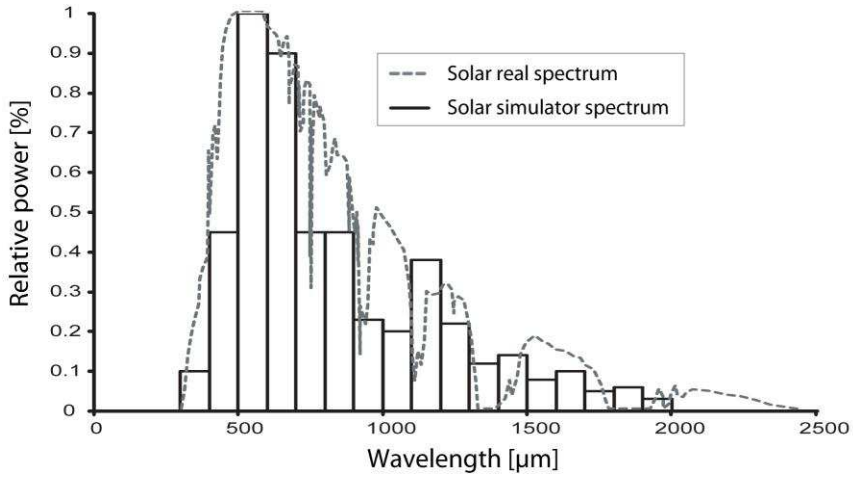

Figure 3. Large scale solar simulator. (Metric units)

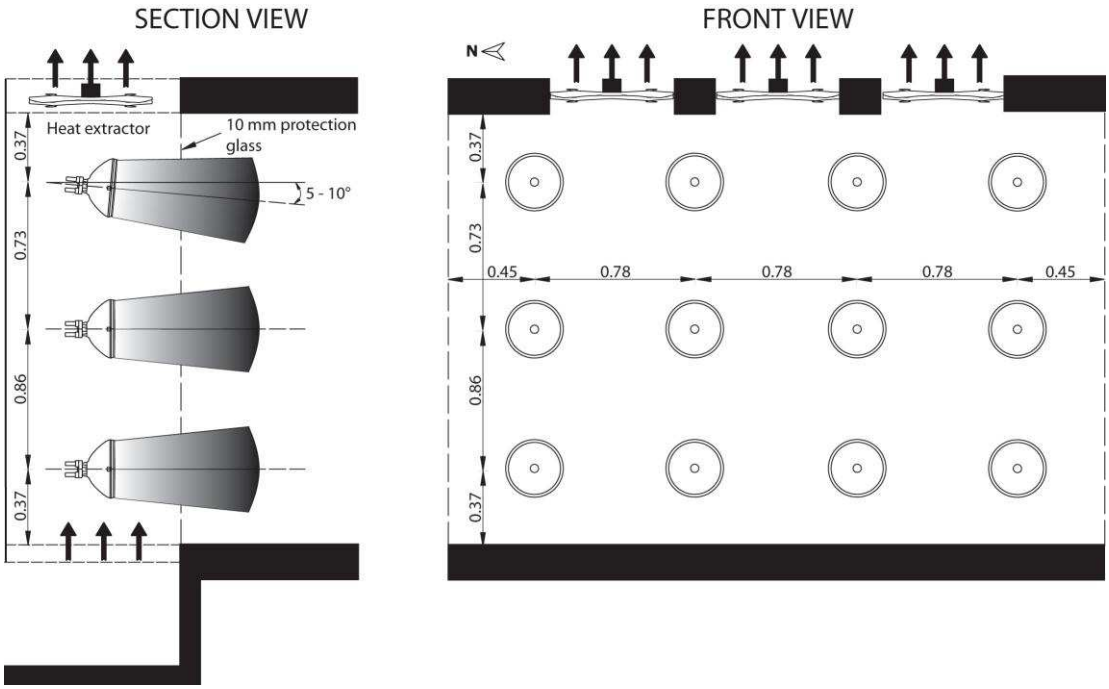

Figure 4. DSF section view: 1, 6 mm glass layer; 2, motorized solar protection; 3, metallic support; 4, solar protection action box; 5, concrete beam; 6, aluminium frame; 7, pane opening articulation; 8, ventilation openings. (Metric units)

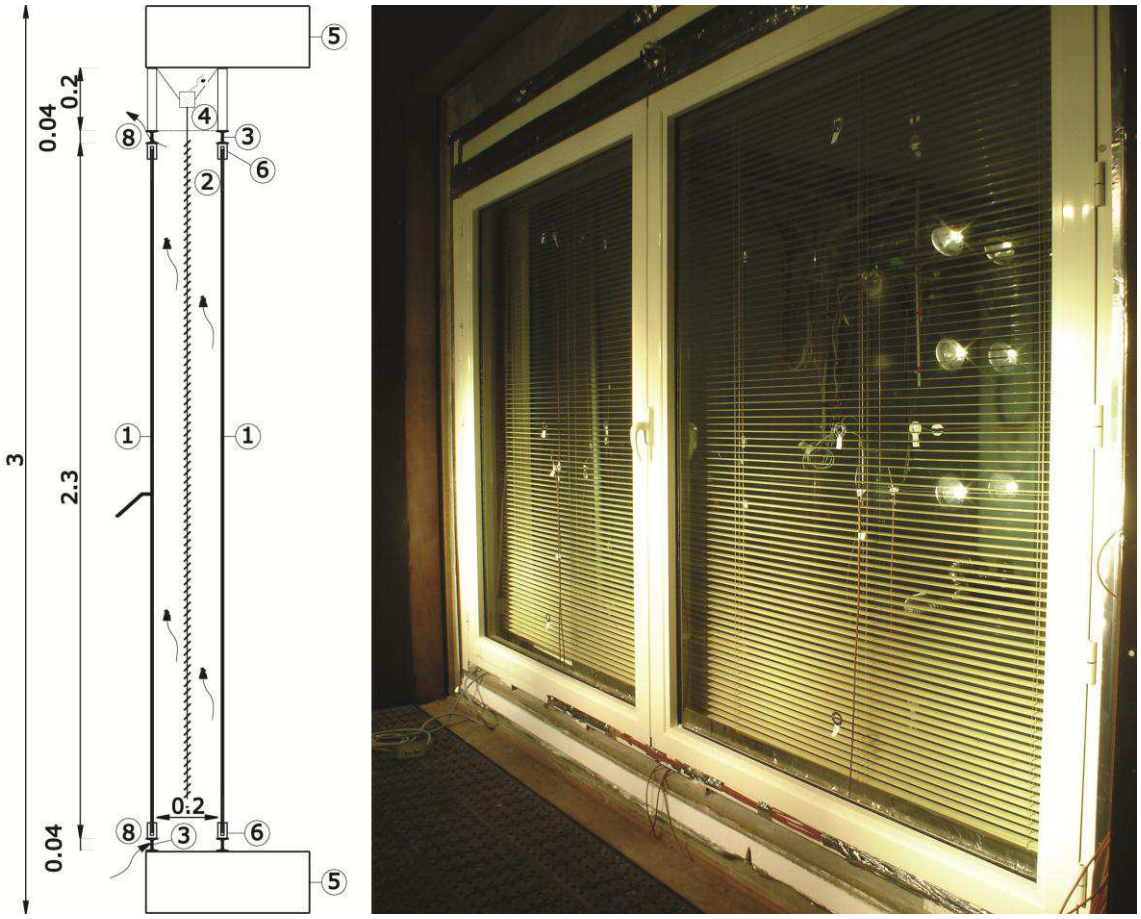

Figure 5. Double-skin façade air supply system. (Metric units)
a) Section view. b) Plan view. c) Flowmeter

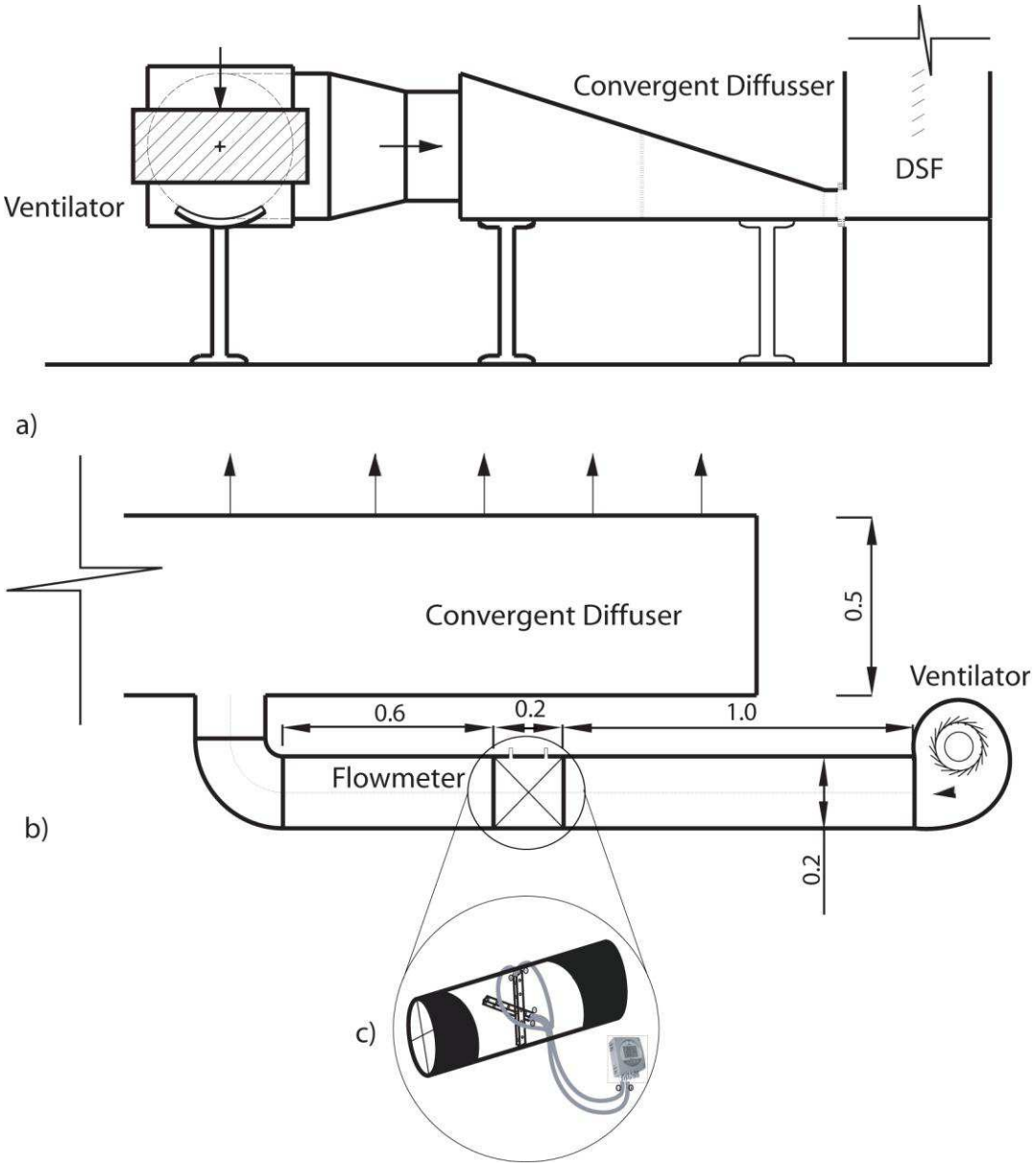

Figure 6. Thermocouples position on double-skin façade elements. (Metric units)

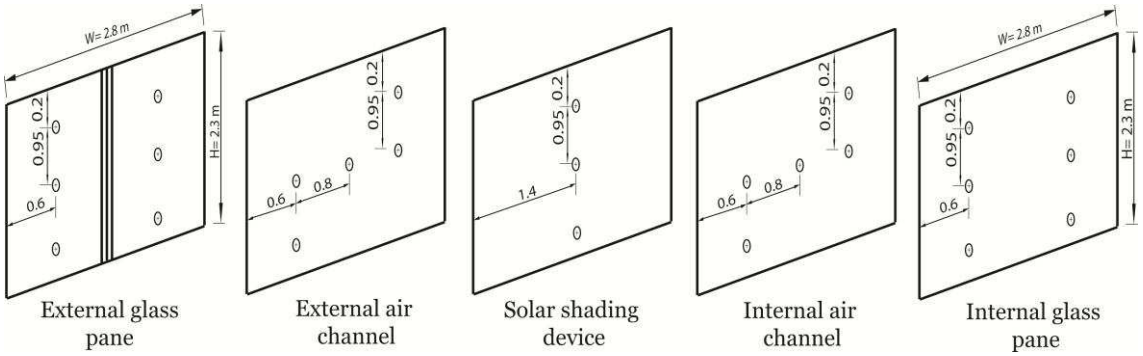

Figure 7. Measurements configurations

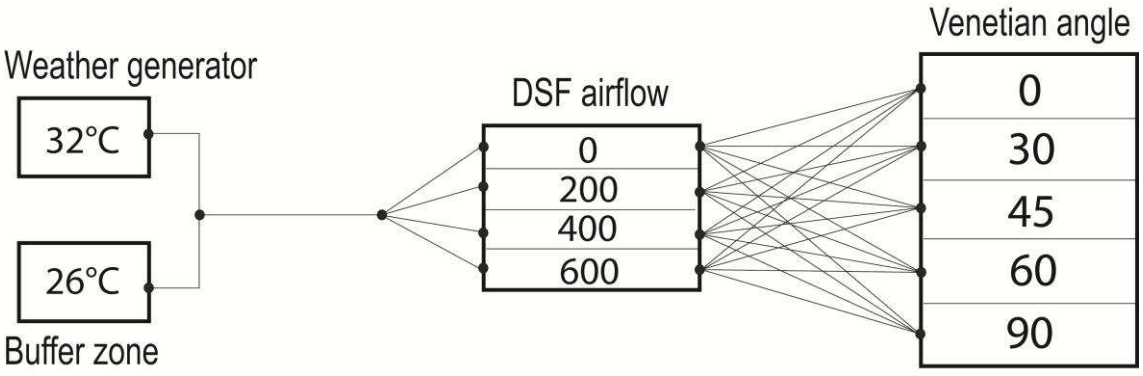

Figure 8. Solar insulation measure grid (external and internal glass). (Metric units)

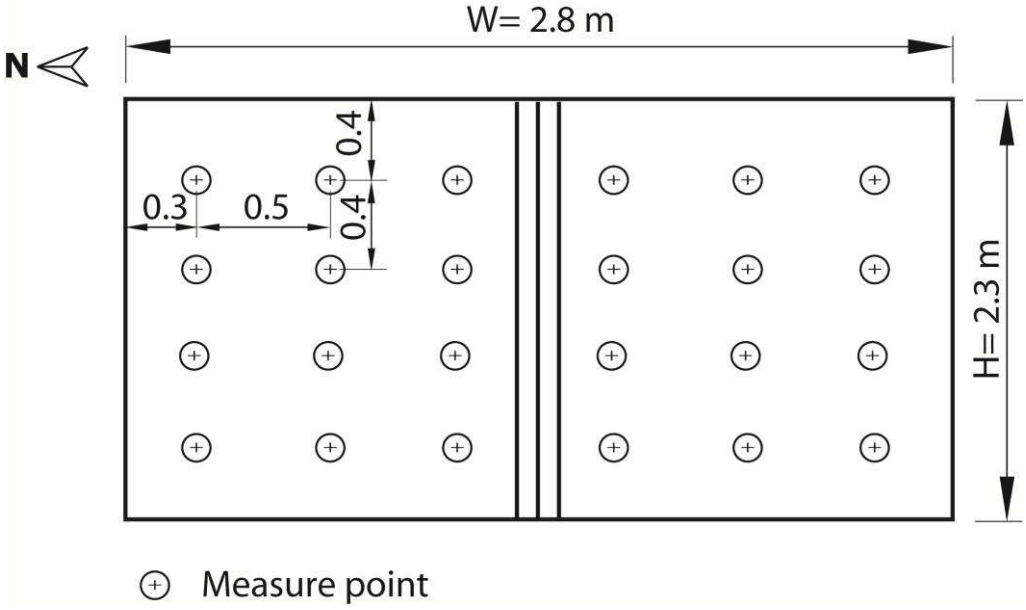

Figure 9. Solar simulator insolation distribution on the external glass pane

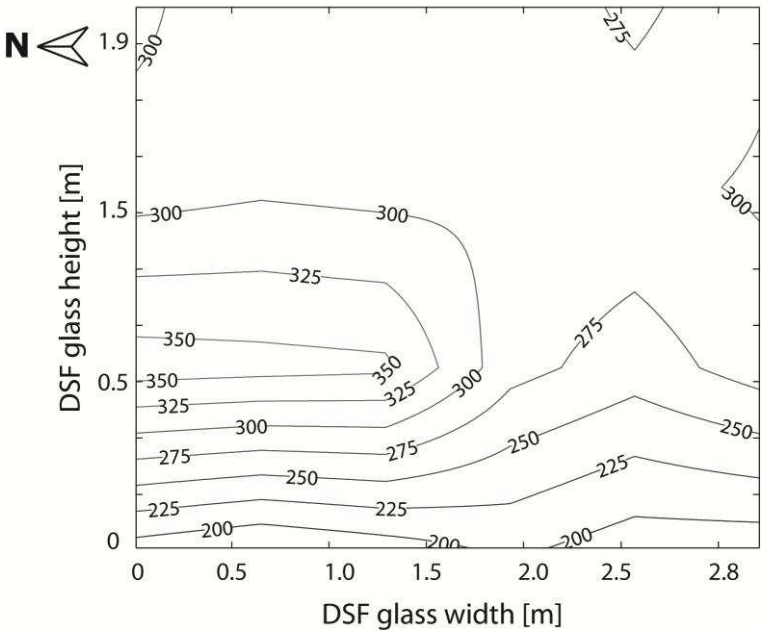

Figure 10. Solar simulator insolation distribution on the internal glass pane (β=0°)

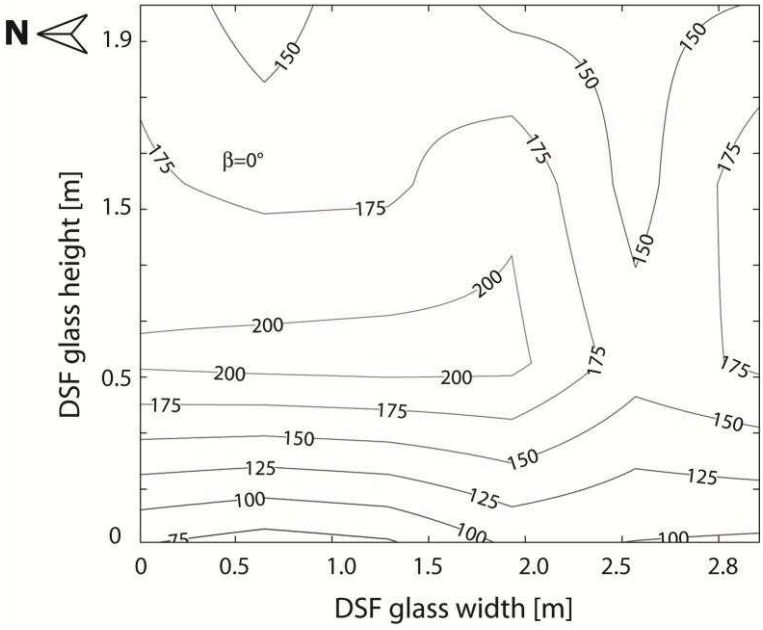

Figure 11. Shading coefficient of the DSF function of different blinds angle

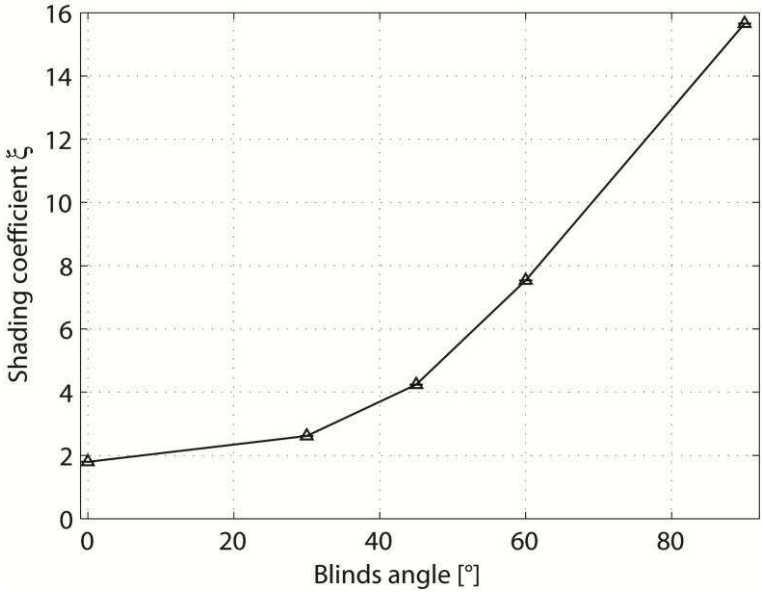

Figure 12. Middle height air velocities inside the façade cavities
a) External cavity; b) Internal cavity;

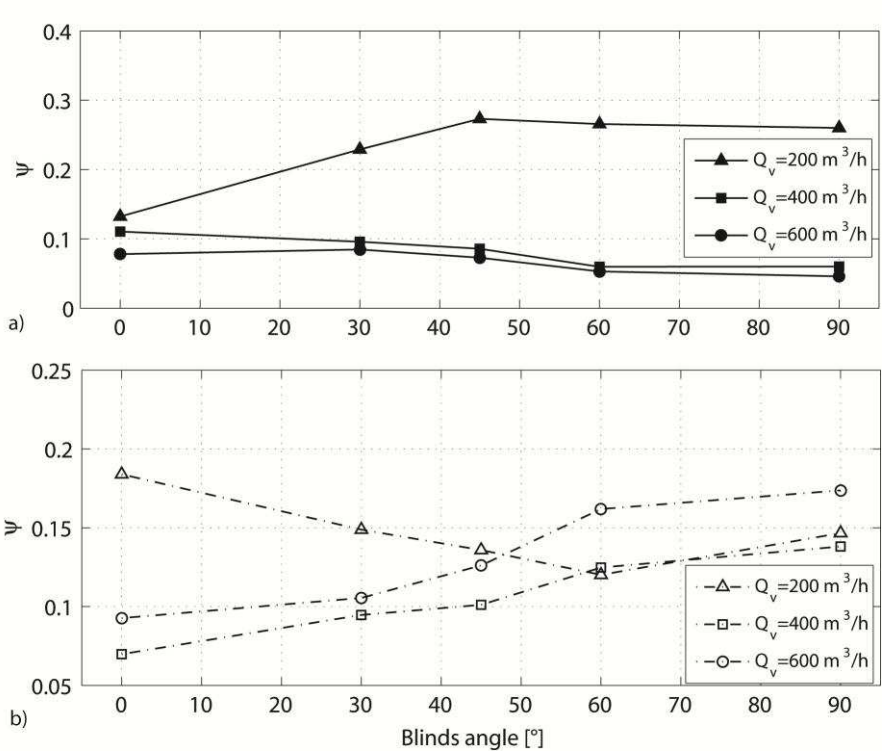

Figure 13. Double-skin façade temperature profile.
a) Blinds at 0° angle (completely opened); b) Blinds at 30° angle; c) Blinds at 45° angle;
d) Blinds at 60° angle; e) Blinds at 90° angle (completely closed);

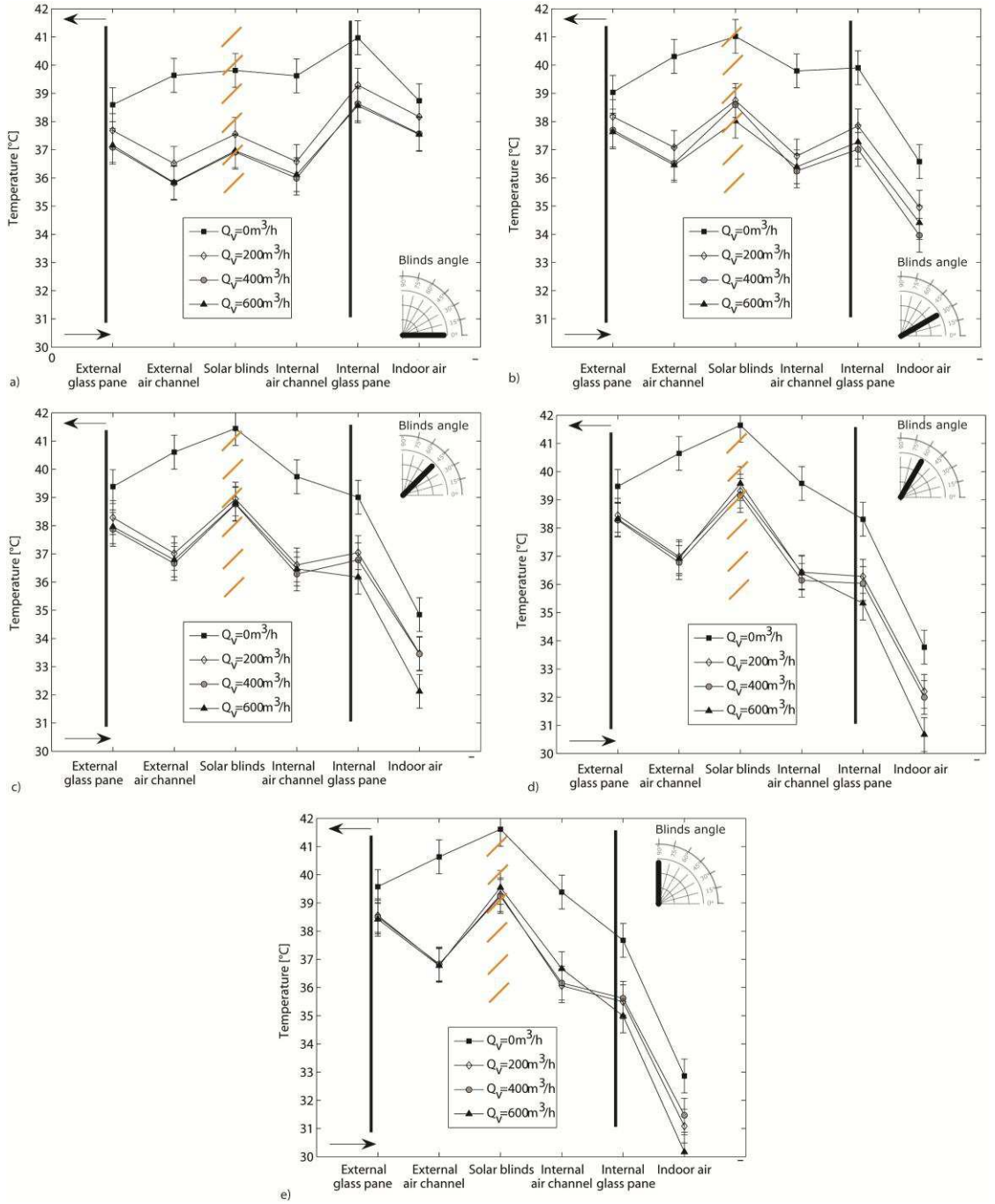

Figure 14. Test cell air temperature

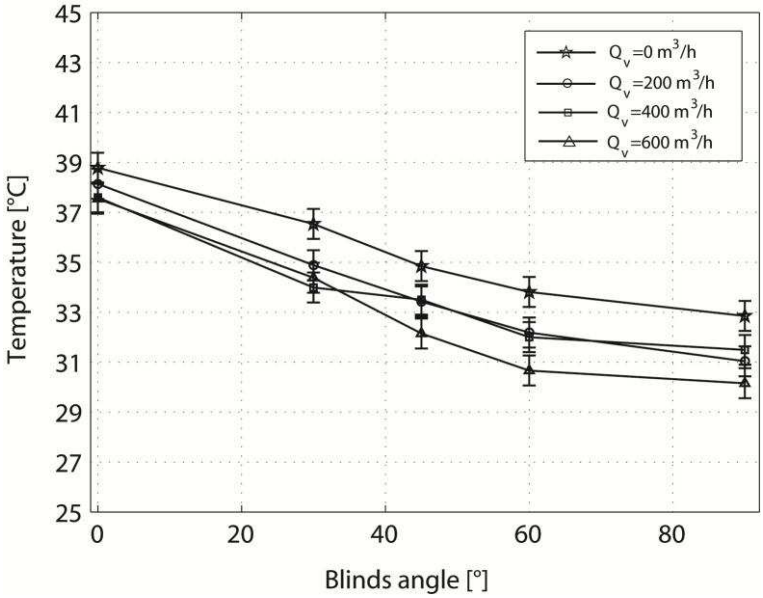

Figure 15. Energy efficiency from the test cell